

Hierarchical Semantic Aggregation for Contrastive Representation Learning

Haohang Xu^{1,2} Xiaopeng Zhang² Hao Li^{1,2} Lingxi Xie² Hongkai Xiong¹ Qi Tian²

¹Shanghai Jiao Tong University, ²Huawei Inc.

{xuhaohang, lihao0374, xionghongkai}@sjtu.edu.cn {zxphistory, 198808xc}@gmail.com tian.qi1@huawei.com

Abstract

Self-supervised learning based on instance discrimination has shown remarkable progress. In particular, contrastive learning, which regards each image as well as its augmentations as a separate class, and pushes all other images away, has been proved effective for pretraining. However, contrasting two images that are de facto similar in semantic space is hard for optimization and not applicable for general representations. In this paper, we tackle the representation inefficiency of contrastive learning and propose a hierarchical training strategy to explicitly model the invariance to semantic similar images in a bottom-up way. This is achieved by extending the contrastive loss to allow for multiple positives per anchor, and explicitly pulling semantically similar images/patches together at the earlier layers as well as the last embedding space. In this way, we are able to learn feature representation that is more discriminative throughout different layers, which we find is beneficial for fast convergence. The hierarchical semantic aggregation strategy produces more discriminative representation on several unsupervised benchmarks. Notably, on ImageNet with ResNet-50 as backbone, we reach 76.4% top-1 accuracy with linear evaluation, and 75.1% top-1 accuracy with only 10% labels.

1. Introduction

As a fundamental task in machine learning, representation learning targets at extracting compact features from the raw data, and has been dominated by the fully supervised paradigm over the past decades [14], [25], [34], [35]. Recent progress on representation learning has witnessed a remarkable success over self-supervised learning [7], [9], [21], [22], [31], which facilitates feature learning without human annotated labels. In self-supervised learning, a network is trained based a series of predefined tasks according to the intrinsic distribution priors of images, such as image colorization [36], rotation prediction [9], context completion [22], *etc.*. More recently, the contrastive learning method [12], which is based on instance discrimination as

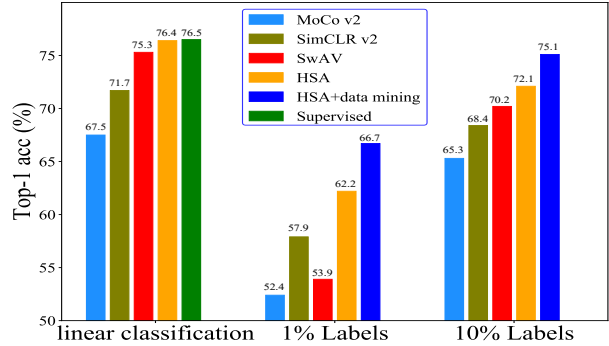


Figure 1. An overall performance comparison of our proposed pre-trained features on several widely evaluated unsupervised benchmarks. Here, a standard ResNet-50 is used as backbone. HSA significantly improves the performance on various tasks.

pretext task, has taken-off as it has been demonstrated to outperform the supervised counterparts on several downstream tasks like classification and detection.

In contrastive learning, due to the lack of labels, each image as well its augmentations is treated as a separate class, and the features among different transformations of an image are pulled closer together, while all other images are treated as negatives and pushed away. In this setting, the invariance is only encoded from low-level image transformations such as cropping, blurring, and color jittering, *etc.*. While the invariance to semantically similar images is not explicitly modeled but on the contrary, they are treated as negatives and pushed away. This is contradictory with the alignment principle [30] of feature representation, which favors the encoders to assign similar features to similar samples. As a result, the optimization is contradictory with the intrinsic distribution of images and suffers slow convergence. This is especially true for the intermediate layers that accept gradients from the last embedding layers.

In order to pursue more discriminative representation, this paper extends the contrastive loss to be compatible with multiple positives during each forward propagation, and thus explicitly models the invariance to semantically similar images. This is achieved by searching the feature representation in the embedding space, and selecting the

nearest neighborhood images that are similar with the anchor for contrastive learning. However, it is a dilemma to select appropriate nearest samples as positives, pulling samples that are *de facto* very similar in the feature space brings about limited performance gain since current representation handles these invariance well, while enlarging the searching space would inevitably introduce noisy samples. To solve this issue, we rely on data mixing to generate extra positive samples, which can be treated as a smoothing version of the anchor. In this way, similar samples are extended in a smoother and robust way, and we are able to better model the intra-class similarity for compact representation.

Training a network that is very deep always remains a challengeable task due to the presence of vanishing gradients, this is especially true under unsupervised paradigm, where the objective is much more opaque comparing with the supervised counterparts. We find that current contrastive learning based methods suffer low discrimination capacity in the intermediate layers, which is harmful for general representation. To solve this goal, we extend the semantic aggregation to earlier layers and propose a hierarchical training strategy that enables the feature representation to be more discriminative throughout the network. This is achieved by explicitly enforcing contrastive loss at intermediate layers as well as the last embedding layers. In this way, the features are deeply supervised throughout the network, which benefits fast convergence and better discriminative power. We find that better semantic aggregation in the middle layers also benefits for transferability.

Our method is reminiscent of the recent proposed Supervised Contrastive Learning [16], which pulls multiple positive samples together. The differences are that, first, SCL is designed for fully supervised paradigm, where the positive samples are simply selected from the ground truth labels, while our method does not rely on these labels, and deliberately design a positive sample selection strategy to facilitate semantic aggregation in a robust way. Second, we extend the contrastive loss to the intermediate hidden layers to enhance the discriminative power of the earlier layers, which is beneficial for discriminative representation and with better transferability, especially for semi-supervised learning.

The proposed hierarchical semantic aggregation strategy significantly boosts the feature representation of contrastive learning when evaluated on several self-supervised learning benchmarks. As shown in Fig. 1, on ImageNet linear evaluation, we achieve 76.4% top-1 accuracy with a standard ResNet-50, which is comparable with the fully supervised counterparts. We set new state-of-the-art results in semi-supervised settings, which achieves 66.7% and 75.1% top-1 accuracy with 1% and 10% labels, respectively. We also validate its transferring ability on several downstream tasks covering detection and segmentation, and achieve better results comparing with previous self-supervised methods.

2. Related Work

Self-supervised representation learning has attracted more and more attentions over the past few years since it is free of labels and is easy to scale up. Self-supervised learning aims at exploring the intrinsic distribution of data samples via constructing a series of pretext tasks, which varies in utilizing different priors of images. Traditional self-supervised learning has sought to learn a compressed code which can effectively reconstruct the input. Among them, a typical strategy is to take advantage of the spatial properties of images, like predicting the relative spatial positions of images patches [7], [21], or inferring the missing parts of images by inpainting [22], colorization [36], or rotation prediction [9] *etc.*. Recent progress in self-supervised learning mainly based on instance discrimination [31], in which each image as well as its augmentations is treated as a separate class. The motivation behind these works is the InfoMax principle, which aims at maximizing mutual information [28], [31] across different augmentations of the same image [3], [12], [28]. The design choices of the InfoMax principle, such as the number of negatives and how to sample them, hyper-parameter settings, and data augmentations all play a critical role for a good representation.

Data augmentation plays a key role for contrastive learning based representation. Since the invariance is only encoded by different transformations of an image. According to [3], [29], the performance of contrastive learning based approaches strongly relies on the types and strength of augmentations, *i.e.*, image transformation priors that do not change object identity. In this way, the network is encouraged to hold invariance in the local vicinities of each sample, and usually more augmentations benefit for feature representation. However, current widely used data augmentation methods are mostly operated within a single sample. One exception is the method in [26], which makes use of mixup mixture for flattened contrastive predictions. However, such a mixture strategy is conducted among all the images, which destroys the local similarity when contrasting mixed samples that are semantic dissimilar.

We are not the first to pull similar samples under unsupervised paradigm. Previous works Deepcluster [1] and local aggregation [37] partially exploring this issue. DeepCluster iteratively groups the features with a standard clustering algorithm, and use the subsequent assignments as supervision to update the network, while local aggregation forces similar data instances to move together in the embedding space, while allowing dissimilar instances to be separated. However, both methods overconfident the similarity computation, which is not robust to noisy samples and limits the further performance gain.

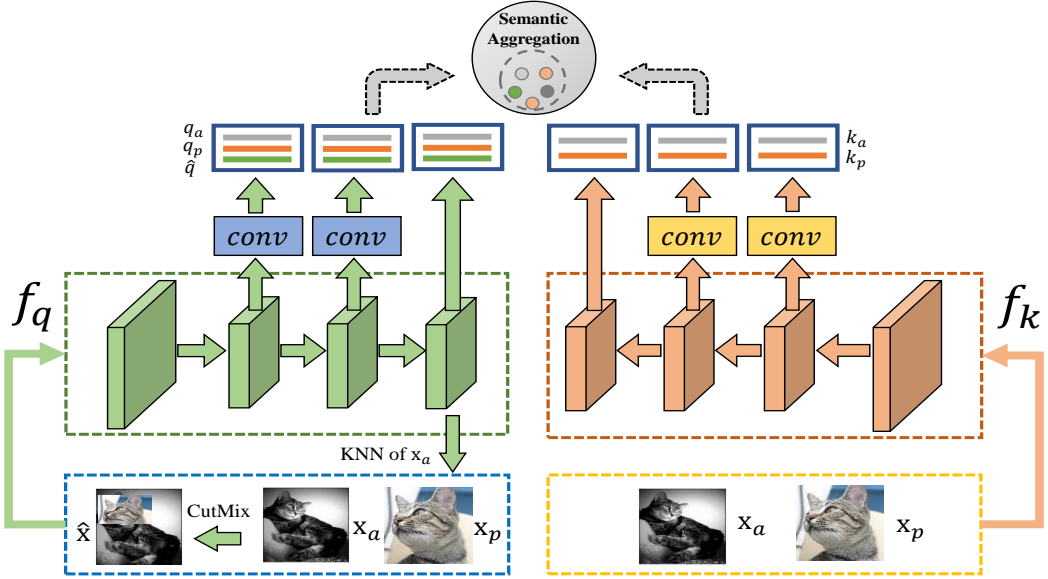


Figure 2. An overview of our proposed hierarchical semantic aggregation framework. The baseline is based on MoCo [12], which requires a query encoder f_q and an asynchronously updated key encoder f_k . Given an anchor image x_a , we randomly select a positive sample x_p from the nearest neighborhood set Ω , and generate the mixed sample \hat{x} . The hierarchical semantic aggregation is enforced by pulling the positive samples x_a , x_p , and \hat{x} in the intermediate layers as well as the last embedding space.

3. Methodology

In this section, we start by reviewing contrastive loss for self-supervised learning, and investigate its drawbacks for general feature representation. Then we present the proposed hierarchical training strategy that pulling semantically similar images at different layers of a network. As shown in Fig. 2, the core idea includes two modules, first, we deliberately design a positive sample selection strategy to expand the neighborhood of a single image, and adjust the contrastive loss to allow for multiple positives during each forward propagation. Furthermore, we propagate the semantic aggregation to the earlier layers to encourage class separability. In this way, the features are trained in a hierarchical way for more compact representation. Each module would be elaborated in the following.

3.1. An Overview of Contrastive Learning

Contrastive learning targets at learning an encoder that is able to map positive pairs to similar representations while pushing away those negative samples in the embedding space. It can be efficiently addressed via momentum contrast [12], which substantially increases the number of negative samples. Given a reference image with two augmented views x and x' , MoCo aims to learn feature representation $q = f_q(x)$ by a query encoder f_q , that can distinguish x' from all other images x_i , where x' and all the negatives x_i are encoded by an asynchronously updated key encoder f_k , with $k^+ = f_k(x')$ and $k_i = f_k(x_i)$, the contrastive loss can

be defined as:

$$\mathcal{L}_q = -\log \frac{\exp(q \cdot k^+ / \tau)}{\sum_{i=0}^K \exp(q \cdot k_i / \tau)}, \quad (1)$$

where τ is the temperature parameter scaling the distribution of distances. However, the positive samples are constrained within a single image with different transformations, and only support one positive sample for each query q , which is low efficient and hard for modeling invariance to semantically similar images.

3.2. Contrastive Learning with Semantic Aggregation

In this section, we describe the proposed positive sample selection strategy and adjust contrastive loss to allow for multiple positives to explicitly model the invariance among similar images.

Positive Sample Selection. For positive samples, we simply make use of k nearest neighbors to search semantically similar images in the embedding space. Specially, given unlabeled training set $\mathcal{X} = \{x_1, x_2, \dots, x_n\}$ and a query encoder f_q , we obtain the corresponding embedding representation $\mathcal{V} = \{v_1, v_2, \dots, v_n\}$ where $v_i = f_q(x_i)$. For a typical Res-50 network, the embedding is obtained from the last average pooled features with dimension 2048. Given an anchor sample x_a , we compute the cosine similarity with all other images, and select the top k samples with the highest similarity as positives $\Omega = \{x^1, x^2, \dots, x^k\}$.

Loss Function. We simply adjust the contrastive loss in Eq. 1 to allow for multiple positives per anchor. Given an anchor sample \mathbf{x}_a and its nearest neighborhood set Ω , we randomly select a positive sample $\mathbf{x}_p \in \Omega$, and the loss function can be reformulated as:

$$\begin{aligned} \mathcal{L}_{q_a} = & -\frac{1}{2} \left(\log \frac{\exp(q_a \cdot k_a / \tau)}{\exp(q_a \cdot k_a / \tau) + \sum_{i=1}^K \exp(q_a \cdot k_i / \tau)} \right. \\ & \left. + \log \frac{\exp(q_a \cdot k_p / \tau)}{\exp(q_a \cdot k_p / \tau) + \sum_{i=1}^K \exp(q_a \cdot k_i / \tau)} \right), \end{aligned} \quad (2)$$

where each anchor sample q_a encoded with f_q , is pulled with two samples k_a and k_q encoded with f_k , and pushed away with all other samples in the key encoder f_k . Symmetrically, for positive sample \mathbf{x}_p , we also have:

$$\begin{aligned} \mathcal{L}_{q_p} = & -\frac{1}{2} \left(\log \frac{\exp(q_p \cdot k_p / \tau)}{\exp(q_p \cdot k_p / \tau) + \sum_{i=1}^K \exp(q_p \cdot k_i / \tau)} \right. \\ & \left. + \log \frac{\exp(q_p \cdot k_a / \tau)}{\exp(q_p \cdot k_a / \tau) + \sum_{i=1}^K \exp(q_p \cdot k_i / \tau)} \right). \end{aligned} \quad (3)$$

The overall loss is the combination of the two losses, which is equipped with two positive samples in the query encoder f_q , and the corresponding two positive samples in the key encoder f_k . Each sample is accompanied with a random data augmentation as described in [5], and is pulled together with all positive samples (also undergo a random data augmentation) from the other encoder.

Expanding the Neighborhood. It is a dilemma to define an appropriate k for nearest sample selection, setting it too small, the objective pulls samples that are already very similar in the feature space, and brings about limited performance gain since current representation handles these invariance well, while setting it too large, it would inevitably introduce noisy samples, and pulling these samples would destroy the local similarity constraint and is harmful for general representation. To solve this issue, we rely on data mixture to expand the neighborhood space of an anchor based on the selected positive samples. The assumption is that the mixed samples act as an interpolation between two samples, and lies in the local neighborhood of the two samples. In this way, the generated mixed samples expand the neighbors in the embedding space that current model cannot handle well, and pulling these samples is beneficial for better generalization.

In particular, we apply CutMix [34] augmentation, which is widely used as a regularization strategy to train neural networks in fully supervised paradigm. Given an anchor sample \mathbf{x}_a , and its positive neighbor $\mathbf{x}_p \in \Omega$, the

mixed sample $\hat{\mathbf{x}}$ is generated as follows:

$$\hat{\mathbf{x}} = \mathbf{M} \odot \mathbf{x}_a + (\mathbf{1} - \mathbf{M}) \odot \mathbf{x}_p, \quad (4)$$

where $\mathbf{M} \in \{0, 1\}^{W \times H}$ is a binary mask that has the same size as \mathbf{x}_a , and indicates where to drop out the region in \mathbf{x}_a and replaced with a randomly selected patch from \mathbf{x}_p , and W, H denotes the width and height of an image, respectively. $\mathbf{1}$ is a binary mask filled with ones, and \odot is the element-wise multiplication operation. For mask \mathbf{M} generation, we simply follow the setting in [34]. Note that different from CutMix used in fully supervised learning that randomly select two images for mixing and change the corresponding labels accordingly, we intentionally sample those similar samples and ensure that the generated samples lie in the local neighborhood of the two samples.

The mixed samples $\hat{\mathbf{x}}$ is treated as a new positive sample, and pulled together with \mathbf{x}_a and \mathbf{x}_p accordingly:

$$\begin{aligned} \mathcal{L}_{\hat{q}} = & -(\lambda \log \frac{\exp(\hat{q} \cdot k_a / \tau)}{\exp(\hat{q} \cdot k_a / \tau) + \sum_{i=1}^K \exp(\hat{q} \cdot k_i / \tau)} \\ & + (1 - \lambda) \log \frac{\exp(\hat{q} \cdot k_p / \tau)}{\exp(\hat{q} \cdot k_p / \tau) + \sum_{i=1}^K \exp(\hat{q} \cdot k_i / \tau)}), \end{aligned} \quad (5)$$

where λ is a combination ratio that determines the cropped area for CutMix operation, and is sampled from beta distribution $\text{Beta}(\alpha, \alpha)$ with parameter α ($\alpha = 1$). The final loss function can be formulated as :

$$\mathcal{L} = \lambda_a \mathcal{L}_{q_a} + \lambda_p \mathcal{L}_{q_p} + \hat{\lambda} \mathcal{L}_{\hat{q}}. \quad (6)$$

We simply set $\lambda_a = \lambda_p = \hat{\lambda} = \frac{1}{3}$ for all the experiments.

3.3. Hierarchical Contrastive Learning

Following training a customized network, the contrastive loss is only penalized at the last embedding layers, while the optimization of the intermediate hidden layers is implicitly penalized by back propagating the gradients to the earlier layers. However, due to the lack of labels, the optimization objective suffers slow convergence rate, and the intermediate layers are especially under fitted and with limited discriminative power comparing with fully supervised learning. Inspired by [17], we extend the proposed contrastive loss in Eq. 6 to the intermediate hidden layers, which targets at explicitly modeling the similarities among image/patches for better discrimination. Specifically, we introduce a companied objective at the end of each stage for a typical ResNet network, which acts as an additional constraint during the learning process. These companied branches are removed after training and hence do not increase complexity of the network.

Table 1. Top-1 accuracy under linear classification on ImageNet with ResNet-50

Method	Accuracy(%)
Supervised	76.5
BigBiGAN[8]	56.6
Local Aggregation [37]	58.8
SeLa [33]	61.5
PIRL [20]	63.6
CPCv2 [15]	63.8
PCL [18]	65.9
SimCLRv2 [4]	71.7
MoCo v2 [5]	71.1
BYOL [11]	74.3
SwAV [2]	75.3
HSA	76.4

As demonstrated in [24], it is too aggressive to directly add a loss layer on the intermediate layers due to the gradient competition issue. For each companied loss at stage l , we add another embedding layer g^l consists of a bottleneck layer and 2 mlp layers before the contrastive loss.

Specifically, given encoder f_q and f_k , we define feature map at stage l as f_q^l and f_k^l , which is truncated at stage l . Each encoder is passed through the embedding layer to encode the intermediate features to a 128-dim vector. The loss function specific to stage l is defined as:

$$\mathcal{L}_{q_a}^l = -\frac{1}{2} \left(\log \frac{\exp(q_a^l \cdot k_a^l / \tau)}{\exp(q_a^l \cdot k_a^l / \tau) + \sum_{i=1}^K \exp(q_a^l \cdot k_i^l / \tau)} + \log \frac{\exp(q_a^l \cdot k_p^l / \tau)}{\exp(q_a^l \cdot k_p^l / \tau) + \sum_{i=1}^K \exp(q_a^l \cdot k_i^l / \tau)} \right), \quad (7)$$

where $q^l = g^l(f_q^l)$ and $k^l = g^l(f_k^l)$, and loss \mathcal{L}_{q_p} and $\mathcal{L}_{\hat{q}}$ can be rewrited to $\mathcal{L}_{q_p}^l$ and $\mathcal{L}_{\hat{q}}^l$ in the same way. So we get the total loss at stage l :

$$\mathcal{L}^l = \frac{1}{3} (\mathcal{L}_{q_a}^l + \mathcal{L}_{q_p}^l + \mathcal{L}_{\hat{q}}^l). \quad (8)$$

When there are L losses corresponding to L intermediate stages, the final losses of the whole network can be computed as:

$$\mathcal{L}_{total} = \mathcal{L} + \sum_{l=1}^L \mathcal{L}^l \quad (9)$$

Table 2. KNN classification accuracy on ImageNet. We report top-1 accuracy with 20 and 200 nearest neighbors, respectively.

Method	20-NN	200-NN
Supervised	75.0	73.2
NPID [31]	-	46.5
LA[37]	-	49.4
PCL[18]	54.5	-
MoCo v2[5]	62.0	59.0
SwAV[2]	59.2	55.8
HSA	72.4	70.7

4. Experiments

In this section, we access our proposed feature representation on several widely used unsupervised benchmarks. We first evaluate the classification performance on ImageNet under linear evaluation and semi-supervised protocols [3], [12]. Then we transfer the representation to several downstream tasks including detection and instance segmentation. We also analyze the performance of our feature representation with detailed ablation studies.

4.1. Pre-training Details

The feature representation is trained based on a standard ResNet-50 [14] network, using ImageNet 2012 training dataset [6]. We follow the settings as in [12], which employs an asynchronously updated key encoder to enlarge the capacity of negative samples, and add a 2-layer MLP on top of the last average pooling layer to form a 128-d embedding vector [5]. The model is trained using SGD optimizer with momentum 0.9 and weight decay 0.0001. The batch size and learning rate are set to 1024 and 0.12 for 32 GPUs, according to the parameters recommended by [5], [10]. The learning rate is decayed to 0 by cosine scheduler [19] during the whole training process.

For companied loss in the intermediate stages, each branch is added with a bottleneck with three layers (1×1 , 3×3 , and 1×1 convolutions, and the number of channels follows the setting of the corresponding stage) and 2-MLP layers. We add the companied loss at both stage 2 and stage 3. For positive sample selection, we perform knn every 5 epochs and select top-10 nearest neighbors for each anchor. For data augmentation, except for those used in [12], we also add multi-crop augmentation [2], which has been demonstrated to be effective for further performance gain. The final model is trained for 800 epochs for evaluation.

4.2. Experiments on ImageNet

Classification with Linear Evaluation. We first evaluate our features by training a linear classifier on top of the

Table 3. Semi-supervised learning by fine-tuning 1% and 10% labeled images on ImageNet. The last row reports results of using a simple data mining procedure.(averaged by 5 trials)

Method	1% labels		10% labels	
	Top-1	Top-5	Top-1	Top-5
Supervised	25.4	48.4	56.4	80.4
UDA[32]	-	-	68.8	88.5
FixMatch[27]	-	-	71.5	89.1
PIRL[20]	30.7	57.2	60.4	83.8
PCL[18]	-	75.6	-	86.2
SimCLR[3]	48.3	75.5	65.6	87.8
MoCo v2[5]	52.4	78.4	65.3	86.6
SwAV[2]	53.9	78.5	70.2	89.9
SimCLRv2[4]	57.9	82.5	68.4	89.2
HSA	62.2	83.0	72.1	90.2
HSA+data mining	66.7	87.7	75.1	92.1

frozen representation, following a common protocol in [12]. The classifier is trained on the global average pooled features of ResNet-50 for 100 epochs, and we report the center crop, top-1 classification accuracy on the ImageNet validation set. As shown in Table 1, the proposed feature representation achieves 76.4% top-1 accuracy, which outperforms the MoCo v2 baseline [5] by 5.3%, and is better than previous best performed result SwAV by 1.1%. Notably, the linear classification accuracy is already on par with the fully supervised counterparts with accuracy of 76.5%.

Classification with KNN Classifier. We also access our representation with KNN classifier, since it does not need to train an additional classifier with labeled data, and is able to evaluate the pretrained features more directly. Following [2], [31], we center crop the images to obtain features from the last average pooled layers, and report the accuracy with 20 and 200 NN in Table 2. For convenient comparison, we also list the KNN classification results of full supervised model, which achieves accuracy of 75.0%. HSA is only 2.6% lower than the supervised baseline, and significantly outperforms previous methods.

Semi-supervised Settings. We also evaluate the representations by fine-tuning with few shot labeled data. Following the evaluation protocol in [3], [4], we fine-tune all layers with only 1% and 10% labeled data. For a fair comparison, we use the same splits of training data as in [3], using SGD optimizer with momentum 0.9 to fine-tune all layers for 60 epochs. The initial learning rate is set to $1e-4$ for backbone and 10 for randomly initialized fc layer.

Table 4. Transfer Learning results on PASCAL VOC detection(averaged by 5 trials)

Methods	AP50	AP75
Supervised	81.4	58.8
MoCo v2 [5]	82.5	64.0
HSA	82.7	64.1

During fine-tuning, only random cropping and horizontal flipping are applied for fair comparisons. Note that our method does not apply any special design like [4] for semi-supervised learning, which makes use of more MLP layers and has shown improved results when fine-tuning with few labels. As shown in Table 3, our method achieves 62.2% top-1 accuracy with only 1% labels and 72.1% top-1 accuracy with 10% labels. In both two settings, our method consistently outperforms other semi-supervised and self-supervised methods, especially when 1% labeled samples are available.

Following semi-supervised learning setting that the unlabeled samples are used for training via assigning pseudo labels, we further conduct data mining to access how the pretrained models improve the data mining procedure. The data mining procedure is conducted as follows: 1) Using the fine-tuned model to infer on all unlabeled samples, and obtaining a confidence distribution for each image. 2) The information entropy is calculated to measure the confidence degree of each image, and we filter those samples with entropy higher than a threshold. 3) Convert the soft labels into one-hot pseudo label via only retaining the highest scored dimension, and train the model together with the ground truth labeled data. We simply set the threshold as 1 and the model is trained following a standard fully supervised learning procedure [14]. Specifically, the model is trained for 90 epoch with initial learning rate set as $1e-4$ for backbone and $1e-2$ for fc layer, and they are both decayed by 0.1 after every 30 epochs. The results are shown in the last row of Table 3, the performance can be further boosted via a simple data mining procedure, and we achieve 66.7% top-1 accuracy with 1% labeled samples, and 75.1% top-1 accuracy with 10% labeled samples. Importantly, with only 10% labels, we are approaching the fully supervised baseline (76.5%) that makes use of all labeled samples.

4.3. Downstream Tasks

We also test the generalization of our unsupervised learned representations on more downstream tasks, including object detection and instance segmentation. All experiments follow MoCo [12] settings for fair comparison.

PASCAL VOC Following evaluation protocol in [12], we use Faster-RCNN [23] detector with R50-C4 backbone. All layers are fine-tuned end-to-end on the union set of

Table 5. Transfer Learning on COCO detection (averaged by 5 trials)

Method	Mask R-CNN,R50-FPN,Det											
	1 x schedule						2 x schedule					
	AP ^{bb}	AP ^{bb} ₅₀	AP ^{bb} ₇₅	AP _S	AP _M	AP _L	AP ^{bb}	AP ^{bb} ₅₀	AP ^{bb} ₇₅	AP _S	AP _M	AP _L
Supervised	38.9	59.6	42.0	23.0	42.9	49.9	40.6	61.3	44.4	25.2	44.4	53.2
MoCo v2 [5]	39.2	59.9	42.7	23.8	42.7	50.0	41.5	62.2	45.3	25.4	44.5	53.3
HSA	40.2	60.9	43.9	24.4	43.9	50.8	42.2	63.0	46.1	26.1	45.6	53.4

Table 6. Transfer Learning on COCO instance segmentation (averaged by 5 trials)

Method	Mask R-CNN,R50-FPN,Seg											
	1 x schedule						2 x schedule					
	AP ^{mk}	AP ^{mk} ₅₀	AP ^{mk} ₇₅	AP _S	AP _M	AP _L	AP ^{mk}	AP ^{mk} ₅₀	AP ^{mk} ₇₅	AP _S	AP _M	AP _L
Supervised	35.4	56.5	38.1	17.5	38.2	51.3	36.8	58.1	39.5	18.9	39.7	53.2
MoCo v2 [5]	35.7	56.8	38.1	17.8	38.1	50.5	37.5	59.1	40.1	19.1	39.8	53.6
HSA	36.5	57.9	39.1	18.5	39.3	51.5	38.1	59.9	40.9	19.5	40.8	53.6

Table 7. Results of adding different modules.

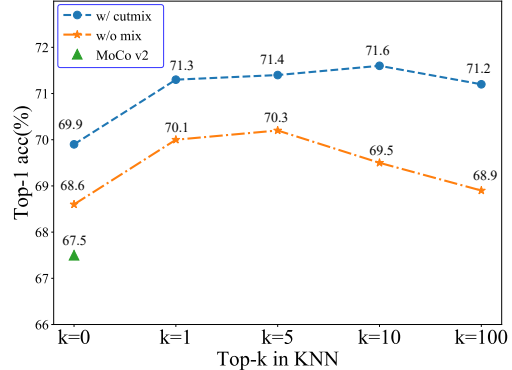
Method	Accuracy(%)
MoCo v2	67.5
$q_a + q_p$	70.3
$q_a + q_p + \hat{q}$	71.6
$q_a + q_p + \hat{q}$ + Multi-Crop	74.6

VOC07+12 for 2 \times schedule, and we evaluate the performance on VOC test07. As shown in Table 4, HSA achieves 82.7% and 64.1% mAP under AP50 and AP75 metric, which is slightly better than the results of MoCo v2.

MS COCO We also evaluate the representation learned on a large scale COCO dataset. Following [12], we use mask R-CNN [13] detector with FPN, fine-tune all the layers end-to-end over the train2017 set, and evaluate the performance on val2017. As shown in Table 5 and Table 6, which compare the detection and segmentation results under 1 \times and 2 \times learning schedule. Our method consistently outperforms the supervised and MoCo v2 baseline. Specifically, in 2 \times schedule, our method surpasses supervised pretrained model by 1.6% and 1.3% under detection and segmentation task, respectively. Notably, we achieve much higher performance on small and medium objects. This is mainly due to the hierarchical aggregation strategy that increases the discrimination power of the intermediate layers.

4.4. Ablation Studies

In this section, we conduct extensive ablation studies to better understand how each component affects the performance. Unless specified, **all results are compared with models trained for 200 epochs without multi-crop data**

Figure 3. Top-1 accuracy with different k in knn.

augmentation, and we report the top-1 classification accuracy under linear evaluation protocol.

Effects of Different Modules. We first diagnose how each component affects the performance, as shown in Table 7, simply add one positive sample q_p boost the baseline MoCo v2 by 2.8%, and introducing mixed samples for pulling further improve the performance by another 1.3%. Following [2], we also adopt multi-crop augmentations, and the performance can be further improved by 3%.

Effects of k in KNN Positive Sample Selection We then inspect the influence when selecting different number of samples as positive candidates. Fig. 3 shows the top-1 accuracy with respect to different k in knn. It can be shown that when no mixed sample is included, the performance is relatively sensitive to k , and the results are relatively robust for a range of k ($k = 1, 5, 10$) when mixed samples are in-

Table 8. Classification accuracy with features of different stages and fine-tuning results with 1% labels.

	Stage2	Stage3	Stage4	1% label
MoCo v2 [5]	44.5	60.2	71.1	52.4
Pull stage4	45.1	60.7	71.6	53.4
Pull stage3&4	45.6	64.0	71.5	54.5
Pull stage2&3&4	46.0	64.0	71.6	54.8

roduced. The reason is that mixed samples act as a strong smoothing regularization, which alleviates the noise introduced by knn selection. We also consider a special case, *i.e.*, always select the same sample, *i.e.*, $\mathbf{x}_p = \mathbf{x}_a$, noted as $k = 0$. This roughly corresponds to enlarging the number of queries, and the result is much lower than selecting similar samples, which demonstrates that the performance improvement is not simply from the increased batch size.

Performance in Shallow Layers. We analyze the performance of the intermediate layers and validate how our proposed hierarchical aggregation strategy benefits the representation. Except for the last layers of stage 4, we also explicitly pull similar samples in earlier layers such as stage 2 and stage 3. Table 8 shows the linear classification accuracy of each stage, it can be shown that pulling similar samples in the shallow layers consistently increases its discrimination power, especially for stage 3, *e.g.*, the accuracy increased by 3.3%, from 60.7% to 64.0%. The performance gain is relatively small in stage 2, partially because the representation in this stage is too low-level, and is hard for global representation. We also note that the performance of the last layers is not significantly affected by penalizing the shallow layer. However, We find that better separability in the shallow layers is beneficial for fine-tuning 1% labels, the accuracy increased by 1.4% when introducing shallow pulling. The advantages of increased representation of shallow layers can be also validated by the downstream detection and segmentation tasks, as shown in Table 5 and Table 6.

Compare with MoCo for Different Training Epochs. In our methods, there are multiple queries during each forward-backward propagation, *i.e.*, \mathbf{x}_a , \mathbf{x}_p , and mixed sample \hat{x} , which is unfair to compare with other methods that only have one query. In order to inspect whether the performance gain is mainly from enlarging the batch size of the query, we compare with MoCo v2 results with more training epochs. As shown in Fig. 4, with 200 training epochs, our method outperforms moco v2 with 600 epochs by 1.1% and even better than moco v2 with 800 epochs. This demonstrates the effectiveness of pulling semantically similar samples and the performance improvement is not simply from increasing the batch size of positive samples.

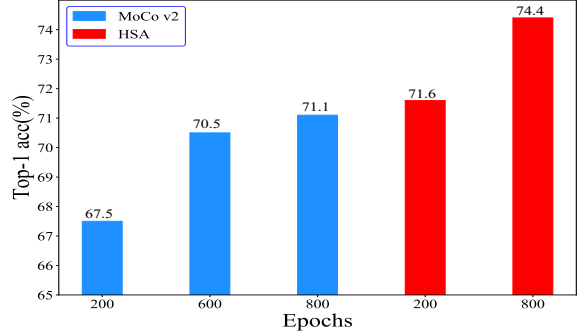


Figure 4. Top-1 accuracy comparisons with different epochs of MoCo v2 and HSA.

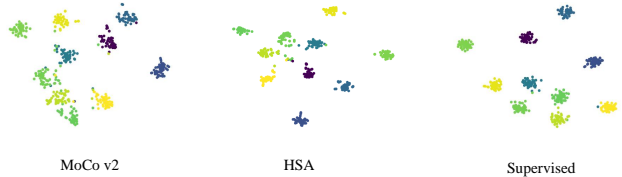


Figure 5. *t-sne* visualization of representation learned by MoCo v2, HSA, and fully supervised learning.

Visualization of Feature Representation We visualize the last embedding feature to better understand the semantic aggregation properties of the proposed method. Specifically, we randomly choose 10 classes from the validation set and provide the *t-sne* visualization of feature representation, supervised training and MoCo v2. As shown in Fig. 5, the same color denotes features with the same label. It can be shown that HSA presents higher aggregation property comparing with MoCo, and the fully supervised learned representation reveals the highest aggregation due to it makes use of image labels.

5. Conclusion

This paper proposed a hierarchical training strategy that pulls semantically similar images for contrastive learning. The main contributions are two folds, first, in order to select similar samples without labels, we deliberately design a sample selection strategy relying on data mixing, which generates new samples that current model does not perform well. The highlight is that samples are only mixed from those similar samples and does not destroy the local similarity structure. Second, we extend the semantic aggregation to intermediate hidden layers and enforces the feature representation to be discriminative throughout the network. In this way, the network can be optimized in a more robust way and we find it is beneficial for general representation. We conduct extensive experiments on widely used self-supervised benchmarks, and consistently outperforms previous self-supervised learning methods.

References

[1] Mathilde Caron, Piotr Bojanowski, Armand Joulin, and Matthijs Douze. Deep clustering for unsupervised learning of visual features. In *Proceedings of the European Conference on Computer Vision (ECCV)*, pages 132–149, 2018. 2

[2] Mathilde Caron, Ishan Misra, Julien Mairal, Priya Goyal, Piotr Bojanowski, and Armand Joulin. Unsupervised learning of visual features by contrasting cluster assignments. *arXiv preprint arXiv:2006.09882*, 2020. 5, 6, 7

[3] Ting Chen, Simon Kornblith, Mohammad Norouzi, and Geoffrey Hinton. A simple framework for contrastive learning of visual representations. *arXiv preprint arXiv:2002.05709*, 2020. 2, 5, 6

[4] Ting Chen, Simon Kornblith, Kevin Swersky, Mohammad Norouzi, and Geoffrey Hinton. Big self-supervised models are strong semi-supervised learners. *arXiv preprint arXiv:2006.10029*, 2020. 5, 6

[5] Xinlei Chen, Haoqi Fan, Ross Girshick, and Kaiming He. Improved baselines with momentum contrastive learning. *arXiv preprint arXiv:2003.04297*, 2020. 4, 5, 6, 7, 8

[6] Jia Deng, Wei Dong, Richard Socher, Li-Jia Li, Kai Li, and Li Fei-Fei. Imagenet: A large-scale hierarchical image database. In *2009 IEEE conference on computer vision and pattern recognition*, pages 248–255. Ieee, 2009. 5

[7] Carl Doersch, Abhinav Gupta, and Alexei A Efros. Unsupervised visual representation learning by context prediction. In *Proceedings of the IEEE international conference on computer vision*, pages 1422–1430, 2015. 1, 2

[8] Jeff Donahue and Karen Simonyan. Large scale adversarial representation learning. In *Advances in Neural Information Processing Systems*, pages 10542–10552, 2019. 5

[9] Spyros Gidaris, Praveer Singh, and Nikos Komodakis. Unsupervised representation learning by predicting image rotations. *arXiv preprint arXiv:1803.07728*, 2018. 1, 2

[10] Priya Goyal, Piotr Dollár, Ross Girshick, Pieter Noordhuis, Lukasz Wesolowski, Aapo Kyrola, Andrew Tulloch, Yangqing Jia, and Kaiming He. Accurate, large mini-batch sgd: Training imagenet in 1 hour. *arXiv preprint arXiv:1706.02677*, 2017. 5

[11] Jean-Bastien Grill, Florian Strub, Florent Altché, Corentin Tallec, Pierre H Richemond, Elena Buchatskaya, Carl Doersch, Bernardo Avila Pires, Zhaohan Daniel Guo, Mohammad Gheshlaghi Azar, et al. Bootstrap your own latent: A new approach to self-supervised learning. *arXiv preprint arXiv:2006.07733*, 2020. 5

[12] Kaiming He, Haoqi Fan, Yuxin Wu, Saining Xie, and Ross Girshick. Momentum contrast for unsupervised visual representation learning. In *Proceedings of the IEEE/CVF Conference on Computer Vision and Pattern Recognition*, pages 9729–9738, 2020. 1, 2, 3, 5, 6, 7

[13] Kaiming He, Georgia Gkioxari, Piotr Dollár, and Ross Girshick. Mask r-cnn. In *Proceedings of the IEEE international conference on computer vision*, pages 2961–2969, 2017. 7

[14] Kaiming He, Xiangyu Zhang, Shaoqing Ren, and Jian Sun. Deep residual learning for image recognition. In *Proceedings of the IEEE conference on computer vision and pattern recognition*, pages 770–778, 2016. 1, 5, 6

[15] Olivier J Hénaff, Aravind Srinivas, Jeffrey De Fauw, Ali Razavi, Carl Doersch, SM Eslami, and Aaron van den Oord. Data-efficient image recognition with contrastive predictive coding. *arXiv preprint arXiv:1905.09272*, 2019. 5

[16] Prannay Khosla, Piotr Teterwak, Chen Wang, Aaron Sarna, Yonglong Tian, Phillip Isola, Aaron Maschinot, Ce Liu, and Dilip Krishnan. Supervised contrastive learning. *arXiv preprint arXiv:2004.11362*, 2020. 2

[17] Chen-Yu Lee, Saining Xie, Patrick Gallagher, Zhengyou Zhang, and Zhuowen Tu. Deeply-supervised nets. In *Artificial intelligence and statistics*, pages 562–570, 2015. 4

[18] Junnan Li, Pan Zhou, Caiming Xiong, Richard Socher, and Steven CH Hoi. Prototypical contrastive learning of unsupervised representations. *arXiv preprint arXiv:2005.04966*, 2020. 5, 6

[19] Ilya Loshchilov and Frank Hutter. Sgdr: Stochastic gradient descent with warm restarts. *arXiv preprint arXiv:1608.03983*, 2016. 5

[20] Ishan Misra and Laurens van der Maaten. Self-supervised learning of pretext-invariant representations. In *Proceedings of the IEEE/CVF Conference on Computer Vision and Pattern Recognition*, pages 6707–6717, 2020. 5, 6

[21] Mehdi Noroozi and Paolo Favaro. Unsupervised learning of visual representations by solving jigsaw puzzles. In *European Conference on Computer Vision*, pages 69–84. Springer, 2016. 1, 2

[22] Deepak Pathak, Philipp Krahenbuhl, Jeff Donahue, Trevor Darrell, and Alexei A Efros. Context encoders: Feature learning by inpainting. In *Proceedings of the IEEE conference on computer vision and pattern recognition*, pages 2536–2544, 2016. 1, 2

[23] Shaoqing Ren, Kaiming He, Ross Girshick, and Jian Sun. Faster r-cnn: Towards real-time object detection with region proposal networks. In *Advances in neural information processing systems*, pages 91–99, 2015. 6

[24] Adriana Romero, Nicolas Ballas, Samira Ebrahimi Kahou, Antoine Chassang, Carlo Gatta, and Yoshua Bengio. Fitnets: Hints for thin deep nets. *arXiv preprint arXiv:1412.6550*, 2014. 5

[25] Olga Russakovsky, Jia Deng, Hao Su, Jonathan Krause, Sanjeev Satheesh, Sean Ma, Zhiheng Huang, Andrej Karpathy, Aditya Khosla, Michael Bernstein, et al. Imagenet large scale visual recognition challenge. *International journal of computer vision*, 115(3):211–252, 2015. 1

[26] Zhiqiang Shen, Zechun Liu, Zhuang Liu, Marios Savvides, and Trevor Darrell. Rethinking image mixture for unsupervised visual representation learning. *arXiv preprint arXiv:2003.05438*, 2020. 2

[27] Kihyuk Sohn, David Berthelot, Chun-Liang Li, Zizhao Zhang, Nicholas Carlini, Ekin D Cubuk, Alex Kurakin, Han Zhang, and Colin Raffel. Fixmatch: Simplifying semi-supervised learning with consistency and confidence. *arXiv preprint arXiv:2001.07685*, 2020. 6

[28] Yonglong Tian, Dilip Krishnan, and Phillip Isola. Contrastive multiview coding. *arXiv preprint arXiv:1906.05849*, 2019. 2

[29] Yonglong Tian, Chen Sun, Ben Poole, Dilip Krishnan, Cordelia Schmid, and Phillip Isola. What makes for

good views for contrastive learning. *arXiv preprint arXiv:2005.10243*, 2020. 2

- [30] Tongzhou Wang and Phillip Isola. Understanding contrastive representation learning through alignment and uniformity on the hypersphere. *arXiv preprint arXiv:2005.10242*, 2020. 1
- [31] Zhirong Wu, Yuanjun Xiong, Stella X Yu, and Dahua Lin. Unsupervised feature learning via non-parametric instance discrimination. In *Proceedings of the IEEE Conference on Computer Vision and Pattern Recognition*, pages 3733–3742, 2018. 1, 2, 5, 6
- [32] Qizhe Xie, Zihang Dai, Eduard Hovy, Minh-Thang Luong, and Quoc V Le. Unsupervised data augmentation for consistency training. *arXiv preprint arXiv:1904.12848*, 2019. 6
- [33] Asano YM., Rupprecht C., and Vedaldi A. Self-labelling via simultaneous clustering and representation learning. In *International Conference on Learning Representations (ICLR)*, 2020. 5
- [34] Sangdoo Yun, Dongyoon Han, Seong Joon Oh, Sanghyuk Chun, Junsuk Choe, and Youngjoon Yoo. Cutmix: Regularization strategy to train strong classifiers with localizable features. In *Proceedings of the IEEE International Conference on Computer Vision*, pages 6023–6032, 2019. 1, 4
- [35] Hongyi Zhang, Moustapha Cisse, Yann N Dauphin, and David Lopez-Paz. mixup: Beyond empirical risk minimization. *arXiv preprint arXiv:1710.09412*, 2017. 1
- [36] Richard Zhang, Phillip Isola, and Alexei A Efros. Colorful image colorization. In *European conference on computer vision*, pages 649–666. Springer, 2016. 1, 2
- [37] Chengxu Zhuang, Alex Lin Zhai, and Daniel Yamins. Local aggregation for unsupervised learning of visual embeddings. In *Proceedings of the IEEE International Conference on Computer Vision*, pages 6002–6012, 2019. 2, 5

Table A.1. Comparisons of Mixup with CutMix augmentation.

Method	Accuracy(%)
MoCo v2	67.5
$q_a + q_p$	70.3
$q_a + q_p + \text{MixUp}(q_a, q_p)$	70.1
$q_a + q_p + \text{CutMix}(q_a, q_p)$	71.6

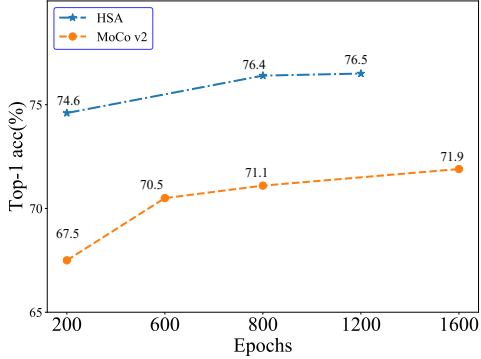


Figure A.1. Top-1 accuracy comparisons for different training epochs of HSA and MoCo v2.

A. Appendix

A.1. MixUp v.s. CutMix augmentations

Besides CutMix, We also consider another cross-sample augmentation strategy Mixup to expand the neighborhood of an anchor. As shown in Table A.1, Mixup is worse than Cutmix, and even slightly worse than baseline method that do not involve any mixed sample in query, *i.e.* $q_a + q_p$ setting, the reason may be that Mixup augmentations destroy the naturality of the pixel distribution.

A.2. The results of more training epochs

To better understand the performance of our proposed HSA method, we train HSA and MoCo v2 for longer epochs to diagnose how the representation evolves for more training epochs. As shown in Fig. A.1, when training for longer epochs, the improvement of HSA is trivial, *i.e.*, only 0.1% improvement when we extend the training epochs from 800 to 1200, the performance tends to converge for HSA. While for MoCo, the performance improves by 0.8% when extending from 800 epochs to 1600 epochs, the convergence rate is rather slow due the pretext task in MoCo that only regards a single image as well as its augmentations as positive samples.

A.3. Performance comparisons of HSA and supervised model

Here we diagnose the performance difference of HSA and fully supervised baseline to uncover the advantages of each model. The performance evaluation is under the linear

classification protocol and we report per-category accuracy. As shown in Fig. A.3, we illustrate the most successful categories of each model, and find that the advantage of supervised model lies in discriminating fine-grained subcategories, *e.g.*, on many sub-classes of dogs (Border collie, Siberian husky, bull mastiff *etc.*). It is intuitive since feature representation among fine-grained sub-categories is very similar, and it is hard to discriminate them without ground truth labels. While for unsupervised model HSA, the most successful categories roughly around categories that require contour information for discrimination, *e.g.* *shopping basket* and *plate rack*, while supervised model usually focuses on discriminative details such as texture. Following the evaluation in Table 2 in the original paper, we also show some example images that use knn for similar samples selection, *i.e.*, given an image in the validation set, and find its top-k nearest neighbors in the training set. The most successful categories of HSA results from capturing the global contour information. This is accordant with the detection results in Table 4 and Table 5 in the original paper, where HSA and MoCo methods achieves much better results on AP75 metric that requires higher localization accuracy.

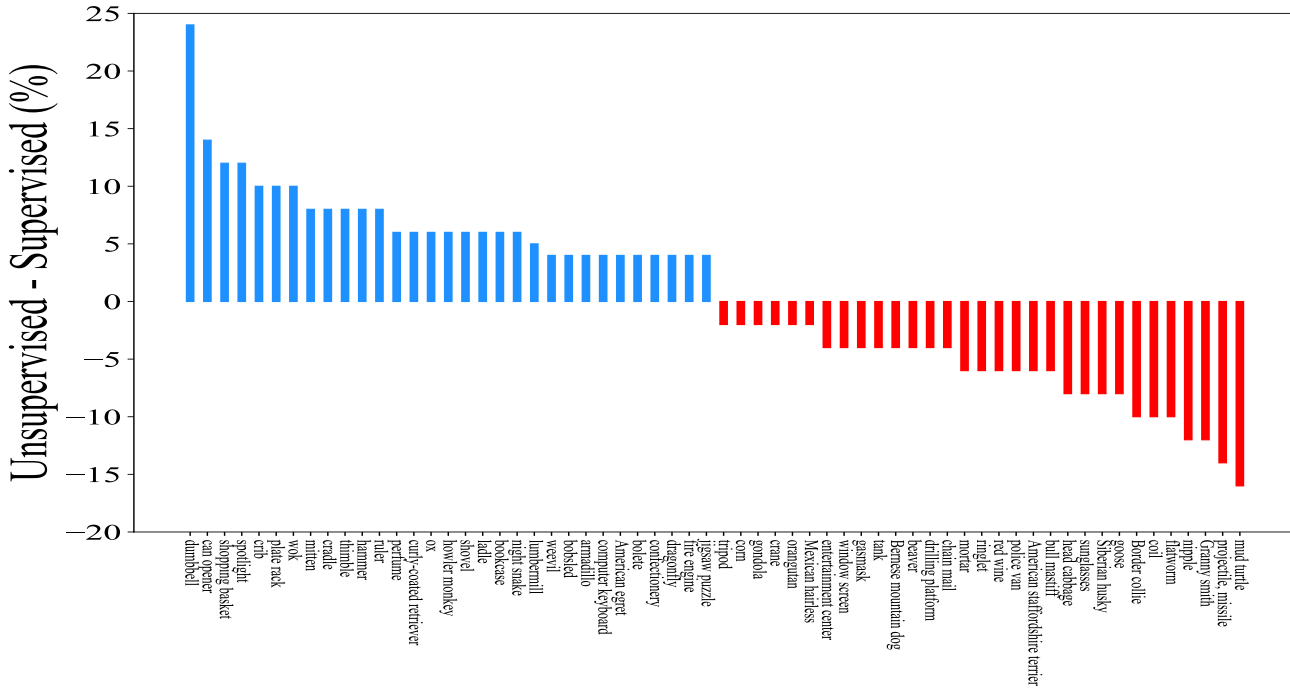


Figure A.2. Top-1 accuracy comparisons on different categories of HSA and fully supervised model. Here we compare most successful categories of each method.



Figure A.3. An illustration of the selected knn samples using HSA and the supervised model.